View metadata, citation and similar papers at core.ac.uk
brought to you by CORE
provided by Institutional Research Information System University of Turin

Powder Technology 208 (2011) 491–495

Contents lists available at ScienceDirect

Powder Technology

journal homepage: www.elsevier.com/locate/powtec

Borosilicate and aluminosilicate pollucite nanocrystals for the storage of radionuclides

Gabriele Montagna [a], Rossella Arletti [a], Giovanna Vezzalini [a], Francesco Di Renzo [b,*]

[a] Dipartimento di Scienze della Terra, Università degli Studi di Modena e Reggio Emilia, Largo S. Eufemia 19, Modena 41100, Italy
[b] Institut Charles Gerhardt Montpellier, UMR 5253 CNRS-UM2-ENSCM-UM1, Ecole Nationale Supérieure de Chimie de Montpellier, 8 rue de l'Ecole Normale, Montpellier 34296, France

ARTICLE INFO

Available online 31 August 2010

Keywords:
Zeolite synthesis
Analcime structure
Nuclear wastes
Solid solution
Isomorphous substitution

ABSTRACT

Cesium can be encapsulated in crystalline aluminosilicates or borosilicates of ANA framework type by hydrothermal synthesis from alkaline solutions at a temperature as low as 115 °C. No miscibility gap is observed in the borosilicate–aluminosilicate solid solution. The presence of cesium in the synthesis batch slightly decreases the yield of incorporation of boron in the silicate framework. Nanocrystals from 25 to 50 nm are formed in most of the synthesis conditions.

© 2010 Elsevier B.V. All rights reserved.

1. Introduction

Several methods for the immobilization of high- and low-level radioactive wastes from reprocessing of nuclear fuel have been developed in the last decades and their optimization is a current research subject. In particular cesium presents a high β activity due to its short-lived isotope ^{137}Cs (half period = 30 years), and a long-lived isotope ^{135}Cs (half period = $2.3*10^6$ years). The specific conditioning of this element should optimize the global management of the package of high-level waste.

Current Portland cement-based technologies for the concentration and immobilization of ^{135}Cs and ^{137}Cs are mainly used for low-level wastes, but often present unsatisfactory leaching behaviour [1], albeit several additives have been proposed to improve their leaching behaviour [2–4]. The borosilicate glass is the most common industrial solution used for the immobilization of high-level waste [5,6]. Moreover other ceramic type materials with different matrices have been used for a durable immobilization of radioactive cesium such as hollandite, perlite and several phosphates [7–9]. These ceramics were prepared using oxide, carbonate and nitrate powders with different cations (Al^{3+}, Cr^{3+}, Ga^{3+}, Fe^{3+}, Mg^{2+}, and Sc^{3+}) of increasing size, in order to evaluate the effect of composition on ceramics microstructure and structure and on cesium incorporation.

The effectiveness of zeolites as cation exchangers and their radiolytic stability have prompted their early application for the remediation of nuclear sites [10–12]. Zeolites are currently used for the removal of cations from high-level alkaline waste solutions [13–15]. The zeolites used for this application, as zeolite A, zeolite X or natural chabasite, erionite, phillipsite and clinoptilolite, present a highly accessible micropore system and a correspondingly fast cation exchange, an asset for cation removal from waste solutions but a drawback for long-term stockage. As a consequence, radionuclide-loaded zeolites are usually vitrified at high temperature to form low-surface area ceramics [16–19].

It has been observed that high-temperature sintering of zeolite A [20] or zeolite Y [21,22] with high cesium loading brings to the formation of crystalline pollucite ceramics with chemical stability better than amorphous glasses previously obtained at lower temperature. Aluminium-rich pollucite is also crystallized in the process of high-temperature sintering of initial glass-bonded zeolite A ceramic waste form (CWF). In the sintering process, cesium-rich zeolite A is transformed in cesiumless sodalite and cesium migrates to newly formed cesium-rich analcime and pollucite phases [23].

The structure of the aluminosilicate framework of pollucite $CsAlSi_2O_6$ does not allow the exchange of the charge-compensating cations [24]. This means that, once Cs^+ cations have been encapsulated by the formation of the aluminosilicate network, their loss is negligible in the stability field of the mineral. This behaviour suggests that direct formation of pollucite in a waste solution would represent a promising method to immobilize cesium cations. Pollucite was early synthesized from cesium-rich alkaline solutions in mild hydrothermal conditions at temperature as low as 160 °C [25].

The present communication reports the preparation of pollucite nanocrystals with composition ranging from aluminosilicate to borosilicate throughout the span of the solid solution $Cs(Al,B)Si_2O_6$. Borosilicate pollucite was earlier crystallized from melts or gels at high temperature (about 900 °C) [26,27] and can be obtained by hydrothermal synthesis at 120 °C [28]. The preparation of nanocrystals presents further advantages, if sintering procedures are needed. These assets could be compensated by the more difficult filtering and

* Corresponding author.
E-mail addresses: gabriele.montagna@unimore.it (G. Montagna), direnzo@enscm.fr (F. Di Renzo).

0032-5910/$ – see front matter © 2010 Elsevier B.V. All rights reserved.
doi:10.1016/j.powtec.2010.08.048

handling of nanocrystals when compared to larger micrometric crystals.

The boro-aluminosilicate nanocrystals whose preparation is dealt with in this communication were prepared as raw materials for experiments intended to verify the effects of crystal size and boron content on cesium incorporation and retention in pollucite. It is important to find a correct B amount that can promote sintering process without increasing the leaching rate. For this reasons, sintering experiments and leaching tests are in progress. It is generally accepted that the leaching behaviour of borosilicate glasses worsens with increasing boron content [29]. Contradictory results [30] can probably be accounted for by the formation of an impervious silica crust by depletion of boron and cations from the rim of samples [31]. However, borosilicate glasses present significant amounts of trigonal boron and polymeric borates [32] and their leaching behaviour does not necessarily correspond to the behaviour of crystalline borosilicate, in which only tetrahedral isolated borates are present.

2. Experimental

Two different silica sources were used: precipitation silica Zeosil 175MP Rhône-Poulenc (Na 0.7 wt.% and Al 0.17 wt.%) or fumed silica Aerosil 200. The other reagents were: boric acid (H_3BO_3) and cesium (CsOH), sodium (NaOH) and aluminium (AlOOH) hydroxides.

The composition of the synthesis batches covered the field of molar ratios $0.22 \leq (B+Al)/Si \leq 0.43$, $0 \leq B/(B+Al) \leq 1$, and $0.10 \leq Cs/(Na+Cs) \leq 1$. The alkalinity ratio ($OH^-/Si$) was higher than 0.64 or lower than 0.37 and the H_2O/Si molar ratio in the range of 0.16–0.22. In a typical synthesis, the appropriate hydroxides were dissolved in deionized water. Boric acid and – later – silica were added to the solution under stirring. The obtained hydrogels were sealed in a stainless steel autoclave and heated in static conditions at a temperature between 115 and 195 °C for a time ranging from 2 to 30 days. The products were filtered, washed with deionized water and dried at 80 °C.

The X-ray diffraction analyses were carried out on a side loaded-sample holder using a Philips PW1729 diffractometer with Bragg–Brentano geometry θ–2θ, CuKα radiation ¼° incident and 0.04 Soller slits. The spectra were collected from 5 to 100° 2θ by using a 0.02° θ step and counting time of 10 s for each step. Rietveld profile fitting was carried out by using the GSAS package [33] with the EXPGUI [34] interface. The structure of Gatta et al. [35] was used as starting model for the refinements. The extracted Bragg peak profiles were modeled by a pseudo-Voight function with 2 refined coefficients (one Gaussian and one Lorentian term, Gw and Ly in GSAS terminology) and a 0.5% cut-off of the peak intensity. The background curve was fitted with a 12 refined coefficient Chebyshev polynomial.

Crystallite size was evaluated from the width of the diffraction lines by the Williamson–Hall method [36,37].

Nine representative synthesized products were chemically analyzed with an ARL-SEMQ electron microprobe operating in the wavelength dispersive (WDS) mode. X-ray counts were converted into oxide weight percentages using the PROBE correction program [38]. To minimize the water loss and cation migration induced by the electron beam, a beam current of 10 nA and a defocused beam of 25 μm were used. The analyses were carried out on carbon coated powder pressed pellets. Only analyses with charge balance error < 10% [39] were considered as being reliable. The batch compositions and the chemical analysis of the products are reported in Table 1.

3. Results and discussion

Crystalline materials with ANA framework type [40] were the only solid products in the whole range of the composition. Fig. 1, where the B/(B + Al) ratio of the synthesis products and of the synthesis batch is reported, shows that in the intermediate terms of the solid solution the yield of incorporation of boron is lower than that of aluminium. Moreover an easier incorporation of Al in the Na-bearing samples is observed.

Table 1
Molar batch composition and chemical analysis of the products for selected syntheses. Tetr: total tetrahedral content (Si + Al + B). Cat: total extra-framework cation content. The EMPA analysis is expressed as formula unit on the basis of 96 oxygen framework atoms.

Synthesis batch				EMPA analysis				
B/(B + Al)	(B + Al)/tetr	Cs/cat	OH^-/Si	Cs	Si	Na	Al	B
0	0.181	0.181	0.80	10.56	34.89	3.45	12.81	0.00
0.511	0.188	0.192	0.73	11.23	35.90	1.58	9.88	1.98
0.995	0.185	0.203	0.67	14.00	31.62	1.40	1.00	15.71
0	0.186	0.977	0.67	11.53	37.38	0.00	10.32	0.00
0.497	0.187	0.977	0.67	12.02	36.72	0.03	7.87	3.15
0.979	0.189	0.976	0.66	14.53	32.46	0.06	0.32	15.53
0	0.300	0.977	0.20	12.02	34.67	0.73	13.52	0.00
0.5	0.230	1	0.67	13.66	35.30	0.06	8.31	4.05
1	0.195	1	0.67	15.51	31.43	0.05	0.05	16.85

The unit cell parameter refinements showed that all samples crystallize in the *Ia* 3*d* space group. This result is in agreement with a disordered Si, Al and B distribution in the tetrahedra. In fact, an ordered distribution of tetrahedral cations would induce a lowering of symmetry.

The cell parameter *a* is reported in Figs. 2 and 3 as a function of the B/(B + Al) ratio in the crystalline products and in the synthesis batches, respectively.

Fig. 2 shows a linear decrease of cell parameter with B/(B + Al) ratio, hence indicating a strong dependence of the cell volume mainly from B content in the tetrahedral positions. The cell parameter decreases from 13.593 Å for the cesium aluminosilicate end-member to 12.985 Å for the cesium borosilicate end-member.

The non-linear variation of the cell parameter with the composition of the synthesis batch (Fig. 3) confirms the discrepancies between the composition of the synthesis batch and the final crystals. Albeit the boron fraction is the main parameter controlling the cell size, the extra-framework cation content also has some effect. Samples synthesized from sodium–cesium mixed synthesis batches systematically present cell parameter slightly higher than the corresponding cesium pure samples (see Figs. 2 and 3).

This effect can be compared with literature data for aluminosilicate pollucite. The cell parameter 13.593 Å found for the cesium aluminosilicate end-member here studied has to be compared with the cell parameters 13.73 for sodium aluminosilicate analcime [41], 13.69 for

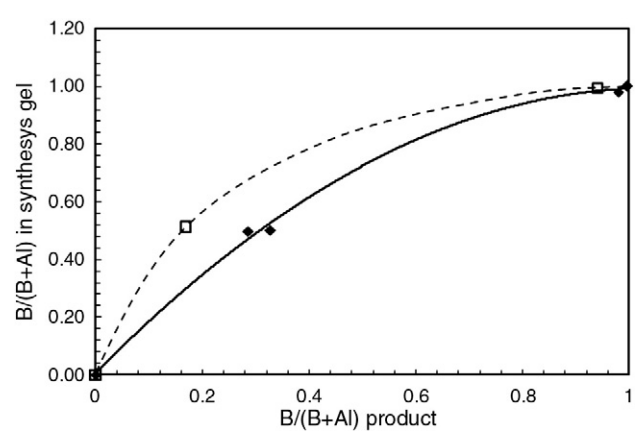

Fig. 1. Boron content in the synthesis batch and in the products. Cs/(Cs + Na) ratios higher than 0.975 (filled lozenges) or lower than 0.33 (void squares).

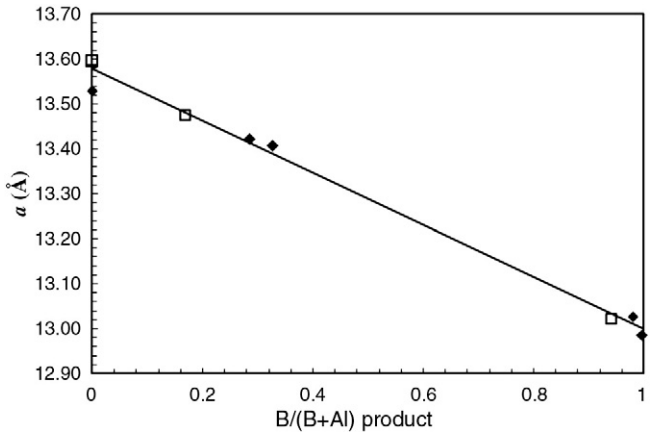

Fig. 2. Cell parameter as a function of the boron content of the crystalline products. Symbols as in Fig. 1.

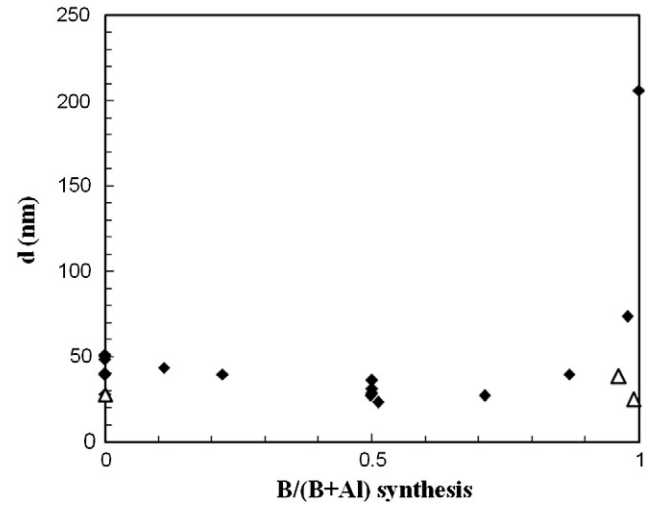

Fig. 4. Crystallite size as a function of the boron content of the synthesis batch. Alkalinity ratios (OH/Si) higher than 0.64 (filled lozenges), lower than 0.37 (void triangle).

natural pollucite with cesium cation fraction (cesium/sum of cations) of 0.75 [42], and 13.672 for pollucite with cesium fraction of 0.886 [43]. To our knowledge, the cell parameter of cesium aluminosilicate pollucite end-member has not yet been published [44].

All these values – from this work and literature – suggest a steady decrease of the cell parameter at increasing cesium content although Cs ionic radius is larger than Na radius. In Cs-bearing ANA phases, Cs is sited in the crystallographic position occupied by the water molecule in natural analcime, (i.e., at the centre of the channel which runs along [111]), where Cs cation coordinates framework oxygen atoms in a distorted octahedron [45]. Moreover Cs is a hydrophobic cation and the water content decreases with its content. Na cation, on the contrary, is located nearer the framework and coordinates both water molecules and framework oxygen atoms [46]. In conclusion, the pollucite cavities are smaller than the analcime ones as an effect of: i) the minor volume occupied by cesium with respect to that occupied by sodium and water and ii) the Cs coordination bonds with only framework oxygen atoms.

The size of the crystallites formed is reported in Fig. 4 as a function of the boron fraction in the synthesis batch. Crystallites are smaller than 50 nm for all compositions except for some of the most boron-rich ones. The smallest crystallites are observed for the intermediate terms of the solid solution, while crystallites larger than 70 nm are only observed for systems with B/(B + Al) greater than 0.98. This trend suggests that the presence of aluminate is a strong nucleation-enhancing factor that hinders the crystal growth, an effect already observed in the synthesis of solid solutions of borosilicate and aluminosilicate zeolite beta [47].

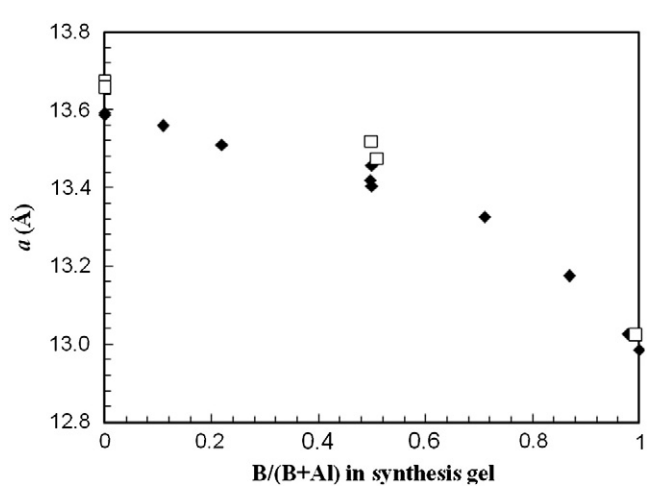

Fig. 3. Cell parameter as a function of the boron content of the synthesis batch. Symbols as in Fig. 1.

Crystallites formed from synthesis batches at low alkalinity are significantly smaller than their analogues formed at higher alkalinity (see Fig. 4). In the case of the boron-rich samples, the solids formed at low alkalinity present a lattice parameter up to 0.08 Å larger than their high-alkalinity analogues, suggesting a lower boron incorporation. For the solids formed in the absence of boron, the cell parameter did not change with the alkalinity of the synthesis batch and the variations in crystallite size cannot be attributed to variations of composition. The observation of smaller crystals at lower alkalinity is quite unusual in zeolite synthesis, the opposite effect being more often observed [48].

Di Renzo et al. [49] observed that the size of sodium aluminosilicate analcime crystals synthesized at 150 °C was systematically larger than 10 μm, several orders of magnitude larger than the size of the crystals obtained in the present study (Fig. 5). Further verifications are needed for the attribution of this large difference in nucleation frequency to the cation ratio Cs/(Cs + Na) alone.

Despite sharing the same structure, analcime and pollucite present significantly different behaviours as far as water mobility and cation exchange are concerned. While analcime presents a water molecule per sodium cation, end-term pollucite is anhydrous. In the intermediate terms of Cs–Na extra-framework composition the water amount is proportional to the sodium content [50]. The absence of reversible dehydration upon heating prevented pollucite to be classified as a zeolite until structural considerations did not prevail on physical macroscopic observations [51]. As far as water and cation mobility is concerned, the behaviour of intermediate cesium–sodium terms could approximate the behaviour of end-term cesium pollucite. Indeed, incorporation of small amounts of cesium or rubidium in an analcime-type zeolite has been shown to highly decrease the water mobility inside the crystal [52,53].

4. Conclusions

The incorporation of cesium cations in ANA framework type materials has been possible in the whole field of composition from aluminosilicate to borosilicate at a temperature as low as 115 °C. Pollucite crystals smaller than 50 nm have been formed at most

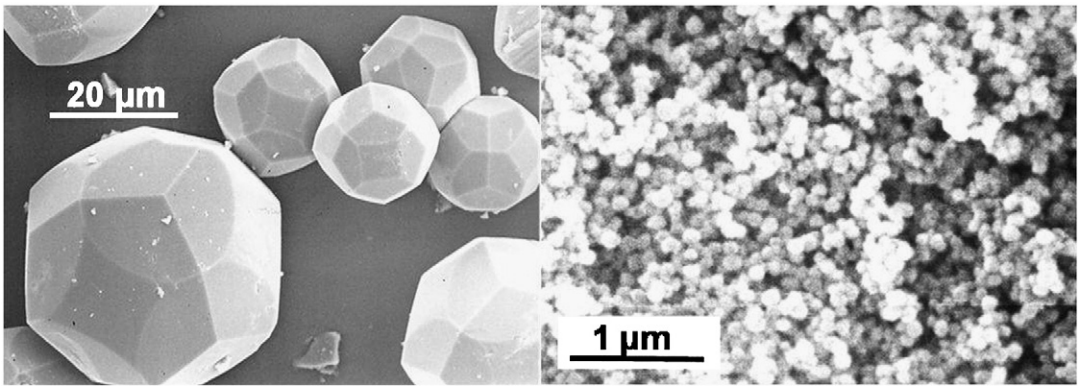

Fig. 5. Micrograph of (lefthand) sodium aluminosilicate analcime synthesized at 150 °C [49] and (righthand) boro-aluminosilicate pollucite synthesized at 120 °C.

compositions of the synthesis batches. The materials formed seem perfectly suited for leaching tests aimed to verify if mild hydrothermal synthesis of cesium silicates is an appropriate method for the immobilization of high-level wastes from plants of treatment of nuclear fuels.

References

[1] S. Bagosi, L.J. Csetenyi, Caesium immobilisation in hydrated calcium-silicate–aluminate systems, Cem. Concr. Res. 28 (1998) 1753–1759.
[2] A.M. El-Kamash, M.R. El-Naggar, M.I. El-Dessouky, Immobilization of cesium and strontium radionuclides in zeolite–cement blends, J. Hazard. Mater. B 136 (2006) 310–316.
[3] G. Bar-Nes, A. Katz, Y. Peled, Y. Zeiri, The mechanism of cesium immobilization in densified silica-fume blended cement pastes, Cem. Concr. Res. 38 (2008) 667–674.
[4] A. Fernandez-Jimenez, D.E. Macphee, E.E. Lachowski, A. Palomo, Immobilization of cesium in alkaline activated fly ash matrix, J. Nucl. Mater. 346 (2005) 185–193.
[5] A.M. Bevilacqua, N.B. Messi de Bernasconi, D.O. Russo, M.A. Audero, M.E. Sterba, A.D. Heredia, Immobilization of simulated high-level liquid wastes in sintered borosilicate, aluminosilicate and aluminoborosilicate glasses, J. Nucl. Mater. 229 (1996) 187–193.
[6] C.P. Kaushik, R.K. Mishra, P. Sengupta, Amar Kumar, D. Das, G.B. Kale, Kanwar Raj, Barium borosilicate glass — a potential matrix for immobilization of sulfate bearing high-level radioactive liquid waste, J. Nucl. Mater. 358 (2006) 129–138.
[7] V. Abin-Chevaldonnet, D. Caurant, A. Dannoux, D. Gourier, T. Charpentier, L. Mézerolles, T. Advocat, Preparation and characterization of (Ba, Cs) (M, Ti)8O16 (M = Al3+, Fe3+, Ga3+, Cr3+, Sc3+, Mg2+) hollandite ceramics developed for radioactive cesium immobilization, J. Nucl. Mater. 366 (2007) 137–160.
[8] J. Balancie, D. Burger, J.-L. Rehspringer, C. Estournès, S. Vilminot, M. Richard-Plouet, A. Boos, Perlite for permanent confinement of cesium, J. Nucl. Mater. 352 (2006) 196–201.
[9] V. Brandel, N. Dacheux, J. Rousselle, M. Genet, Synthesis of some new thorium phosphates, C. R. Chim. 5 (2002) 599–606.
[10] M. Calligaris, A. Messetti, G. Nardin, L. Randaccio, Crystal structures of the hydrated and dehydrated forms of a partially cesium-exchanged chabazite, Zeolites 6 (1986) 137–141.
[11] S. Komarmeni, R. Roy, Use of γ-zirconium phosphate for Cs removal from radioactive waste, Nature 299 (1982) 707.
[12] N.F. Chelishchev, Use of natural zeolites at Chernobyl, in: D.W. Ming, F.A. Mumpton (Eds.), Natural Zeolites '93. Occurrence, Properties, Use, International Committee of Natural Zeolites, New York, 1993, pp. 525–532.
[13] B. De Gennaro, A. Colella, P. Aprea, C. Colella, Evaluation of an intermediate-silica sedimentary chabazite as exchanger for potentially radioactive cations, Microporous Mesoporous Mater. 61 (2003) 159–165.
[14] P. Ackerman, T.R. Johnson, L.S.H. Chow, E.L. Carls, W.H. Hannum, J.J. Laidler, Treatment of waste in the IFR fuel cycle, Prog. Nucl. Energy 31 (1997) 141–154.
[15] M.Y. Khalil, E. Merz, Immobilization of intermediate-level wastes in geopolymers, J. Nucl. Mater. 211 (1994) 141–148.
[16] D.H. Siemens, D.E. Knowlton, Vitrification of highly loaded SDS zeolites, in: G.H. Bryan (Ed.), Trans. Am. Nucl. Soc., 43, 1982, pp. 148–149.
[17] S. Bulbulian, P. Bosch, Vitrification of gamma irradiated $^{60}Co^{2+}$ zeolites, J. Nucl. Mater. 295 (2001) 64–72.
[18] P. Bosch, D. Caputo, B. Liguori, C. Colella, Safe trapping of Cs in heat-treated zeolite matrices, J. Nucl. Mater. 324 (2004) 183–188.
[19] F. Iucolano, B. Liguori, L. Sabová, E. Chmielewskà, D. Caputo, C. Colella, Safe trapping of Cs in heat-treated zeolite matrices. Part 2, Stud, Surf. Sci. Catal. 174 (2008) 537–540.
[20] R. Dimitrijevic, V. Dondur, N. Petranovic, The high temperature synthesis of $CsAlSiO_4$–ANA, a new polymorph in the system Cs_2O–Al_2O_3–SiO_2, J. Solid State Chem. 95 (1991) 335–345.
[21] R.L. Bedard, E.M. Flanigen, High density leucite/pollucite based ceramics from zeolites, U.S. Pat. 5 (1993) 192–722.
[22] R.L. Bedard, E.M. Flanigen, R. von Ballmoos, et al., Zeolite as ceramics: engineering new and novel ceramic compositions and microstructures from molecular sieves, Proceedings of the 9th International Zeolite Conference, Montreal 1992, Butterworth-Heinemann, 1993, pp. 667–674.
[23] M.J. Lambregts, S.M. Frank, Characterization of cesium containing glass-bonded ceramic waste forms, Microporous Mesoporous Mater. 64 (2003) 1–9.
[24] R.M. Barrer, J.W. Baynham, N. McCallum, Hydrothermal chemistry of silicates. Part V. Compounds structurally related to analcite, J. Chem. Soc. (1953) 4035–4041.
[25] R.M. Barrer, N. McCallum, Hydrothermal chemistry of silicates. Part IV. Rubidium and cesium aluminosilicates, J. Chem. Soc. (1953) 4029–4034.
[26] S.A. Gallagher, G.J. McCarthy, Preparation and X-ray characterization of pollucite ($CsAlSi_2O_6$), J. Inorg. Nucl. Chem. 43 (1981) 1773–1777.
[27] D. Mazza, M. Lucco-Borlera, On the substitution of Fe and B for Al in the pollucite ($Cs^{141}Si_2O_6$) structure, J. Eur. Ceram. Soc. 17 (1997) 1767–1772.
[28] F. Di Renzo, M. Derewinski, G. Chiari, J. Plévert, M.F. Driole, F. Fajula, P. Schulz, Insertion of boron in tectosilicate frameworks in the presence of large alkali cations, Microporous Mater. 6 (1996) 151–157.
[29] A. Ledieu, F. Devreux, P. Barboux, L. Sicard, O. Spalla, Leaching of borosilicate glasses. I. Experiments, J. Non-Cryst. Solids 4 (2004) 3–12.
[30] D.L. Moir, A. Chatt, Studies on leaching behavior of sodium borosilicate glasses by neutron-activation effects of groundwater composition, pH, surface-area to volume ratio, and temperature, J. Radioanal. Nucl. Chem. 161 (1992) 503–526.
[31] F. Devreux, A. Ledieu, P. Barboux, Y. Minet, Leaching of borosilicate glasses. II. Model and Monte-Carlo simulations, J. Non-Cryst. Solids 4 (2004) 1–25.
[32] M.E. Fleet, S. Muthupari, Coordination of boron in alkali borosilicate glasses using XANES, J. Non-Cryst. Solids 255 (1999) 233–241.
[33] A.C. Larson, R.B. Von Dreele, General Structure Analysis System (GSAS), Report LAUR 86-748, Los Alamos National Laboratory, Los Alamos, 2000.
[34] B.H. Toby, EXPGUI, a graphical user interface for GSAS, J. Appl. Cryst. 34 (2001) 210–213.
[35] G.D. Gatta, F. Nestola, T.B. Ballaran, Elastic behavior, phase transition, and pressure induced structural evolution of analcime, Am. Miner. 91 (2006) 568–578.
[36] G.K. Williamson, W.H. Hall, X-ray line broadening from filed aluminium and wolfram, Acta Metall. 1 (1953) 22–31.
[37] P. Karen, P.M. Woodward, Liquid-mix disorder in crystalline solids: $ScMnO_3$, J. Solid State Chem. 141 (1998) 78–88.
[38] J.J. Donovan, M.L. Rivers, PRSUPR — a PC based automation and analysis software package for wavelength-dispersive electron-beam microanalysis, Microbeam Anal. (1990) 66–68.
[39] E. Passaglia, The crystal chemistry of chabazites, Am. Miner. 55 (1970) 1278–1301.
[40] Ch. Baerlocher, W.M. Meier, D.H. Olson, Atlas of Zeolite Framework Types, Elsevier, Amsterdam, 2007.
[41] G. Gottardi, E. Galli, Natural Zeolites, Springer, Berlin, 1986 76.
[42] R.M. Beger, The crystal structure and chemical composition of pollucite, Z. Kristallogr. 129 (1969) 280–302.
[43] P. Černý, F.M. Simpson, The Tanco Pegmatite at Bernic Lake, Manitoba; X, Pollucite, Can. Mineral. 16 (1978) 325–333.
[44] D.K. Teerstra, P. Černý, First natural occurrence of end-member pollucite: a product of low-temperature reequilibration, Eur. J. Mineral. 7 (1995) 1137–1148.
[45] R.S. Bubnova, N.K. Stepanov, A.A. Levin, S.K. Filatov, P. Paufler, D.C. Meyer, Crystal structure and thermal behaviour of boropollucite $CsBSi_2O_6$, Solid State Sci. 6 (2004) 629–637.
[46] F. Mazzi, E. Galli, Is each analcime different? Am. Mineral. 63 (1978) 448–460.
[47] M. Derewinski, F. Di Renzo, P. Espiau, F. Fajula, M.A. Nicolle, Synthesis of zeolite beta in boron–aluminium media, Stud. Surf. Sci. Catal. 69 (1991) 127–134.

[48] F. Di Renzo, Zeolites as tailor-made catalysts: control of the crystal size, Catal. Today 41 (1998) 37–40.
[49] F. Di Renzo, F. Fajula, P. Espiau, M.A. Nicolle, R. Dutartre, The influence of microgravity on zeolite crystallization, Zeolites 14 (1994) 256–261.
[50] R.M. Barrer, N. McCallum, Intracrystalline water in pollucite, Nature 167 (1951) 1071.
[51] D.S. Coombs, A. Alberti, T. Armbruster, G. Artioli, C. Colella, E. Galli, J.D. Grice, F. Liebau, J.A. Mandarino, H. Minato, E.H. Nickel, E. Passaglia, D.R. Peacor, S. Quartieri, R. Rinaldi, M. Ross, R.A. Sheppard, E. Tillmanns, G. Vezzalini, Recommended nomenclature for Zeolite minerals: report of the subcommittee on zeolites of the International Mineralogical Association, Commission on New Minerals and Mineral Names, Mineral. Mag. 62 (4) (1998) 533–571.
[52] A. Dyer, A.M. Yusof, Diffusion in heteroionic analcimes: Part 1. Sodium–potassium–water system, Zeolites 7 (1987) 191–196.
[53] A. Dyer, A.M. Yusof, Diffusion in heteroionic analcimes: Part II. Diffusion of water in sodium/thallium, sodium/lithium, and sodium/ammonium analcimes, Zeolites 9 (1987) 129–135.